Electronic Supplementary Material (ESI) for RSC Advances.

Electronic Supporting Information

Triazatruxene Radical Cation: A Trigonal Class III Mixed Valence System

Tony George Thomas,[†] Sarap Chandra Shekar,[‡] Rotti Srinivasamurthy Swathi[‡*] and Karical Raman Gopidas[†*]

[†]Photosciences and Photonics, Chemical Sciences and Technology Division
CSIR-National Institute for Interdisciplinary Science and Technology (CSIR-NIIST)
Thiruvananthapuram – India.

[‡]School of Chemistry, Indian Institute of Science Education and Research
Thiruvananthapuram (IISER-TVM), Kerala, India.

Contents

1. General Experimental Procedures

The electronic absorption spectra were recorded on a Shimadzu 3101PCUV-Vis-NIR Scanning spectrophotometer and Agilent-8453 Diode array spectrophotometer. Redox potentials of the amines were recorded using a BAS CV50W voltammetric analyzer. Solutions of the amines (1×10^{-3} M) in acetonitrile containing 0.1 M tetra-n-butylammonium hexafluorophosphate as supporting electrolyte were thoroughly de-aerated before use. A Pt disc electrode was used as working electrode and a platinum wire was used as counter electrode and the potentials were referenced to saturated calomel electrode (SCE). Spectroelectrochemical measurements were carried out using a Pt mesh electrode in a 1 mm quartz cuvette. ^{1}H NMR spectra were recorded in $CDCl_3$ on a Bruker Avance II 500 spectrometer at ambient temperature; chemical shifts are reported relative to TMS in ppm by referencing to the residual solvent signals. Spectroscopic grade acetonitrile purchased from Aldrich was used for spectroscopic and electrochemical measurements.

2. Characterization Data for TAT

Yield: 10%. ^{1}H NMR (500 MHz, $CDCl_3$) δ 8.57 (d, J = 8 Hz, 3 H), 7.70 (d, J = 8.5 Hz, 3 H), 7.58 (t, J = 8 Hz, 3 H), 7.47 (t, J = 7.5 Hz, 3 H), 4.56 (s, 9 H) ppm. HRMS (m/z): 387.1 (M^+).

3. Cyclic and Square Wave Voltammograms of TAT

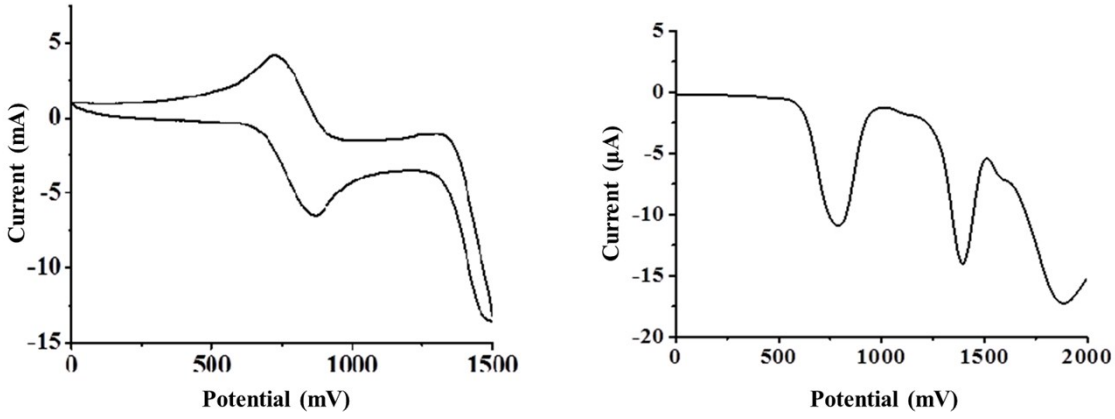

Figure S1: Cyclic and square wave voltammograms of TAT.

4. Simulated EPR Spectrum of $TAT^{\cdot+}$

The EPR spectrum of $TAT^{\cdot+}$ was simulated using EasySpin[1], version 5.0.22, for MATLAB R2014a[2]. The experimental parameters included the data points corresponding to magnetic field and their respective intensities, the microwave frequency (9.69 GHz) and the temperature (298 K). g-value used was 2.01. Simulation was performed using the EasySpin function pepper for the solid-state CW EPR spectrum. A comparison of the experimental and the simulated EPR spectra is shown in Figure S2.

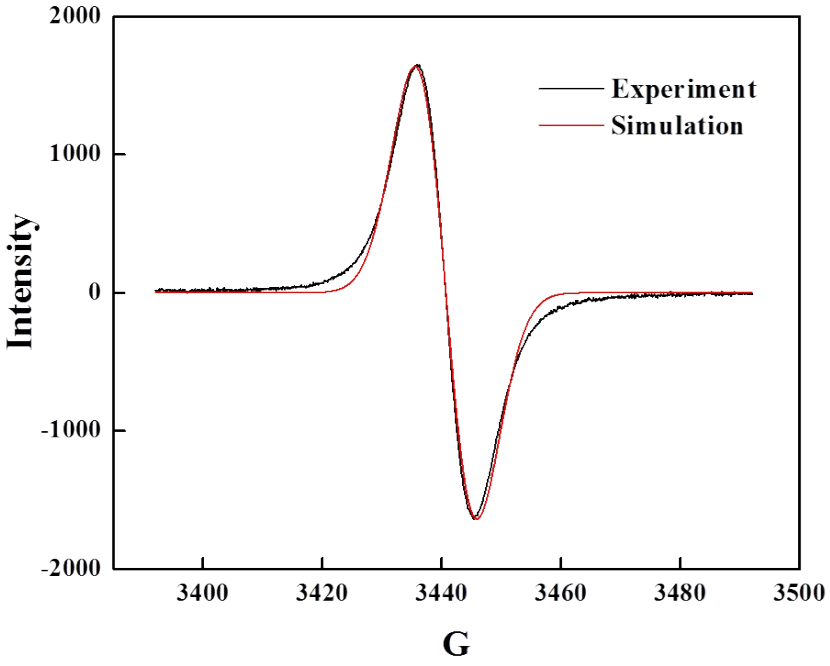

Figure S2: A comparison of the experimental and the simulated EPR spectra of $TAT^{\cdot+}$.

5. Three-state Models

Tri-nuclear organic mixed valence systems like $TAT^{\bullet+}$ could be modelled using three-state models. A semiclassical model to describe the potential energy surfaces (PES) in such systems was earlier proposed by Launay and Babonneau (LB model), subsequent to which Cannon et al. (Cannon model) reported an alternative approach to obtain the PES. Here, we employ both the models to describe the PES for a class III delocalized tri-nuclear mixed valence system.

LB Model:

The PES contours shown in Figures 3 and 5 are obtained using equation 1 of ref. 33.

Adiabatic potential energy curves can then be obtained by performing a transformation from the (q_2, q_3) variables to the (r, θ) variables and then taking a cross-section of the resultant surfaces in the θ = 0 plane. On performing the transformation from the (q_2, q_3) variables to the (r, θ) variables as defined by $q_2 = r\cos\theta$ and $q_3 = r\sin\theta$, the e_a, e_b and e_c terms in equation 1 of ref. 33 are transformed as

$$e_a = \frac{1}{2}r^2 - \sqrt{\frac{2}{3}}\, r\, cos\theta$$

$$e_b = \frac{1}{2}r^2 - \sqrt{\frac{1}{2}}\, r\, sin\theta + \sqrt{\frac{1}{6}}\, r\, cos\theta$$

$$e_c = \frac{1}{2}r^2 + \sqrt{\frac{1}{2}}\, r\, sin\theta + \sqrt{\frac{1}{6}}\, r\, cos\theta.$$

The cross-sections of the above surfaces in the θ = 0 plane yield

$$U_1^{'} = \frac{1}{2}r^2 - \sqrt{\frac{2}{3}}\, r$$

$$U_2^{'} = \frac{1}{2}r^2 + \sqrt{\frac{1}{6}}\, r$$

$$U_3^{'} = \frac{1}{2}r^2 + \sqrt{\frac{1}{6}}\, r\,.$$

The diabatic potential energy curves obtained using the above equations are shown in Figure 6.

The resultant potential energy matrix thus obtained

$$V = \begin{bmatrix} U_1^{'} & B & B \\ B & U_2^{'} & B \\ B & B & U_3^{'} \end{bmatrix}$$

can now be diagonalized for a given value of 'B' to obtain the adiabatic potential energy curves:

$$E_a^{'} = \frac{1}{12}\left(6B - \sqrt{6}\,r + 6r^2 - \sqrt{324B^2 + 36\sqrt{6}\,B\,r + 54\,r^2}\right)$$

$$E_b^{'} = \frac{1}{12}\left(6B - \sqrt{6}\,r + 6r^2 + \sqrt{324B^2 + 36\sqrt{6}\,B\,r + 54\,r^2}\right)$$

$$E_c^{'} = \frac{1}{6}\left(-6B + \sqrt{6}\,r + 3r^2\right).$$

Thus, for $TAT^{\bullet+}$ using the above equations, the adiabatic curves for the cases B = 0.0 and B = -0.41 are obtained and are shown in Figure 6. The energies are reported as $E^{'}$ in reduced units. For the sake of clarity, individual potential energy curves are shown in Figure S3 and Figure S4.

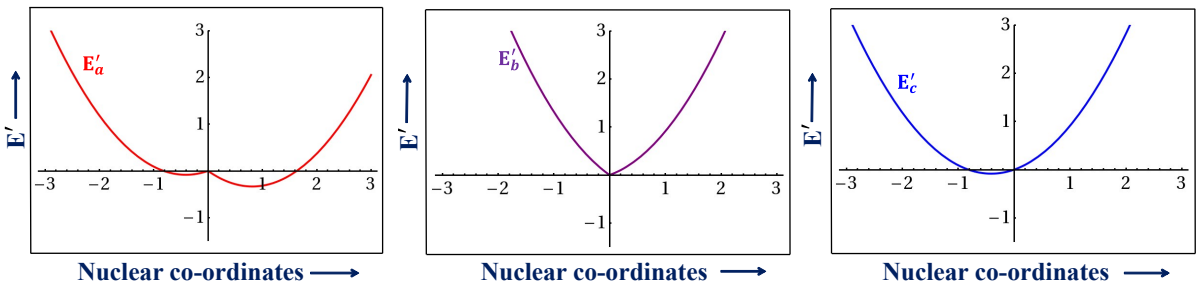

Figure S3: Potential energy curves as a function of the nuclear co-ordinates for the adiabatic states ($E_a^{'}, E_b^{'}\ and\ E_c^{'}$) of $TAT^{\bullet+}$ for B = 0 (localization).

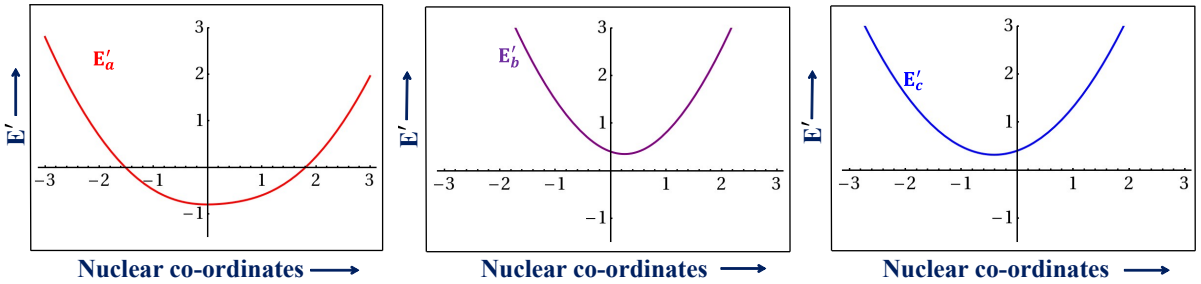

Figure S4: Potential energy curves as a function of the nuclear co-ordinates for the adiabatic states ($E_a^{'}, E_b^{'}\ and\ E_c^{'}$) of TAT$^{\bullet+}$ for B = -0.41 (delocalization).

Cannon Model:

The diabatic and the adiabatic potential energy curves corresponding to c=0 are obtained using equations 8-9 and 12-13 of ref. 34 and are shown in Figure 4. Again, as earlier, individual potential energy curves are shown in Figure S5. All the numerical calculations for the three-state models are performed using Mathematica[3].

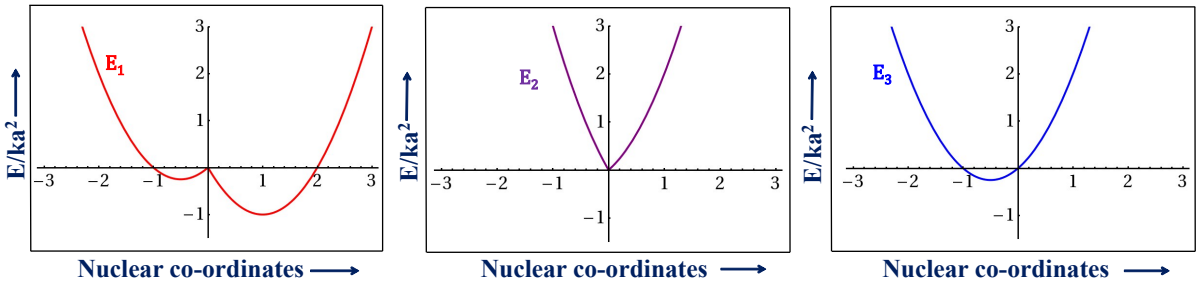

Figure S5: Potential energy curves as a function of the nuclear co-ordinates for the adiabatic states (E_1, E_2 and E_3) of TAT$^{\bullet+}$ when c = 0 (localization).

6. Computational Details

Electronic structure calculations were performed for TAT$^{\bullet+}$ in acetonitrile solvent using density functional theory at the B3LYP/6-311G(d,p) level using the Gaussian 09 suite of programs.[4] The optimized geometry of TAT$^{\bullet+}$ is shown in Figure 2A. The electronic absorption spectrum has been computed using the TDDFT method at the same level and is shown in Figure 2C along with the experimental absorption spectrum.

7. EPR Spectrum of $TAT^{\cdot+}$ Computed using DFT

We also calculated the EPR spectrum of $TAT^{\cdot+}$ using DFT. Initially, using the optimized geometry of $TAT^{\cdot+}$, we calculate the nuclear properties of $TAT^{\cdot+}$, namely hyperfine coupling parameters (isotropic part, dipolar part, 2nd order contribution to hyperfine coupling), electric field gradients, electron densities at the nuclei in ACN at the B3LYP/6-311G(d,p) level using the ORCA program[5]. The resultant output parameters are imported into EasySpin program to calculate the EPR spectrum. For $TAT^{\cdot+}$, if we assume that the radical is delocalized equally on all nitrogens and if we consider hyperfine interactions due to all the three nitrogens and the hydrogens of the methyl groups, the total number of lines expected in the hyperfine spectrum would be $(2\times3\times1+1)(2\times9\times1/2+1) = 7\times10 = 70$ lines. Therefore, the EPR spectrum is computed considering that the lone electron couples to 3N and 9H of the methyl groups in $TAT^{\cdot+}$. Simulation was performed at the experimental microwave frequency (9.69 GHz) and at a linewidth of 0.05 mT using the EasySpin function garlic for computing the CW EPR spectra of radicals in solution and the resultant spectrum is shown below:

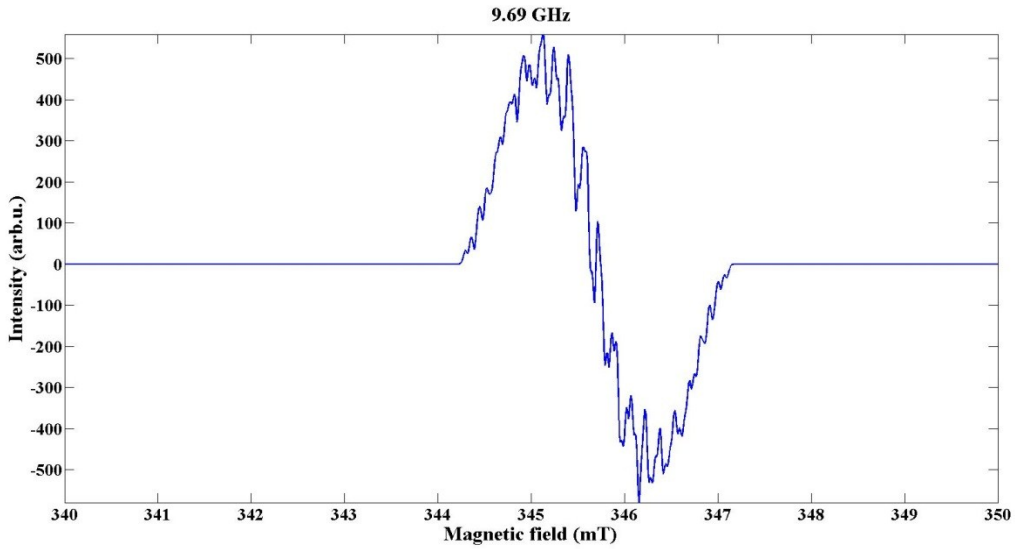

Figure S6: Computed EPR spectrum of $TAT^{\cdot+}$.

8. References

1. Stoll S., Schweiger A. EasySpin, a Comprehensive Software Package for Spectral Simulation and Analysis in EPR. *J. Magn. Reson.,* **2006**, 178, 42-55.

2. MATLAB, Release 2014a, The MathWorks, Inc., Natick, Massachusetts, United States, **2014**.
3. Mathematica, version 7.0; Wolfram Research, Inc.: Champaign, IL, **2008**.
4. Frisch, M. J.; et al. Gaussian 09; Gaussian, Inc.: Wallingford, CT, **2009**.
5. F. Neese, "The ORCA Program System," *WIREs Comput. Mol. Sci.,* **2012**, 2, 73–78.